

Non-linear Distributed Optical-fibre Sensing

A. J. Rogers

Department of Electronic and Electrical Engineering,
King's College London,
Strand, LONDON WC2R 2LS

ABSTRACT

Distributed Optical-Fibre Sensing (DOFS) offers full information on the spatial and temporal behaviour of a large number of measurand fields. Among potential applications are the monitoring and control of any large structure (including 'smart' systems), and a range of environmental monitoring requirements.

Methods for realizing DOFS hitherto have relied, almost exclusively, on linear backscatter techniques. A notable exception is the Raman temperature measurement system, which relies on non-linear backscatter. New explorations are concerned to investigate the possibility of utilising other non-linear effects in either backscatter or forward-scatter arrangements. Forward-scatter methods utilise the non-linear interaction between counter-propagating light signals in a single-mode optical fibre; these hold promise for markedly improved signal levels, with consequent measurement accuracies of $\sim 1\%$, and spatial resolutions $\sim 0.1\text{m}$ over distances up to 1km.

Attention recently has concentrated on the use of the optical Kerr effect. Two ways in which this effect may be used in DOFS will be described. Recent experimental results will be presented and remaining problems will be defined.

1. INTRODUCTION

Distributed Optical-Fibre Sensing (DOFS) provides the means by which the spatial and temporal behaviour of a range of physical fields may be determined. A variety of methods for implementing DOFS has been explored, each, as always is the case, with its own set of advantages and disadvantages [1,2].

Research in DOFS is stimulated by a number of important applications. For example, the requirement to measure the distribution of temperature in equipments vulnerable to 'hot-spots' or to anomalous temperature gradients, such as power transformers or multilayered material structures; the requirement to measure strain distributions in critical structures such as pressure vessels, boilers, dams, bridges, tall buildings; and the requirement to locate, spatially, anomalously large electric and/or magnetic disturbances in malfunctioning electrical and electronic equipment. More recently, the growing interest in structures which, effectively, have the ability to self-monitor, and perhaps also to self-adjust ('smart' structures), has provided added impetus to DOFS research [3].

The optical fibre possesses singular advantages for distributed sensing : it is dielectric, insulating, flexible and sensitive (in its optical propagation properties) to a wide range of external physical fields. Its flexible, 'one-dimensional' nature makes it very suitable for the variety of geometrical configurations needed for distributed sensing in myriad industrial applications.

Additionally, some emphasis should be placed on the potential importance of DOFS in research and in manufacturing diagnostics. Here the importance lies largely with its ability to probe the behaviour of systems more satisfactorily as a result of access to more detailed spatial and temporal information, and to detect and locate departures from prescribed behaviour with much greater facility.

2. BACKSCATTER VERSUS FORWARD-SCATTER DOFS

Most DOFS explorations to date have relied on backscatter arrangements [1-4]. In these, a pulse of light is launched into an optical fibre and is continuously Rayleigh backscattered as it propagates (fig 1). Time resolution of the emerging backscattered light then reveals the spatial distribution of any external field which is capable of modulating, in a deterministic way, some characterizing property of the light, this latter being demodulated by the detector. Such a one-dimensional 'lidar' arrangement has the clear advantage of simplicity, but it has a number of disadvantages.

The primary disadvantage is that Rayleigh backscatter is at a low level, of order 10^{-5} of the forward travelling energy, per unit length of fibre. Moreover, since the fibre attenuation (in a propagation 'window') will depend almost entirely on Rayleigh scatter, there will be an optimum length, for a given scatter coefficient, with regard to both sensitivity and resolution of the DOFS system.

This can be given some quantification by examining the backscatter power equation:

where:
$$p(t) = \frac{c}{2} \cdot E_0 \alpha s \exp(-\alpha ct) \quad - (1)$$

$p(t)$ is the backscattered power at time t .
 c is the speed of light in the fibre.
 α is the attenuation coefficient.
 s is the backscatter capture fraction.
 E_0 is the launch pulse energy.

From this it is easy to see that the optimum fibre length is given by

$$L = \frac{1}{\alpha}$$

and hence that the power received from the far end is given by:

$$P_L = \frac{cE_0 s}{2Le} \quad ; \quad (e = \exp(1))$$

Now if we require a spatial resolution of ΔL at distance L from the launch end, it is clear, firstly, that the launched pulse width must be less than ΔL . Secondly, the achievable resolution is limited by the detector signal-to-noise ratio (SNR) :-

the energy received from ΔL at L is given by :

$$\delta E_L = P_L \cdot \frac{2\Delta L}{c} = \frac{E_0 s}{e} \cdot \frac{\Delta L}{L} \quad - (2)$$

Suppose that we need to measure the measurand to an accuracy (i.e. fractional error) of η , over ΔL . If we assume that the detector is operating to the shot noise limit (Poisson statistics) we have that:

$$\frac{\delta E_L}{h\nu} > \frac{1}{\eta^2}$$

where ν is the optical frequency and h is Planck's constant.

Hence, using (2) :

$$\Delta L \geq \frac{eLh\nu}{E_0 s} \cdot \frac{1}{\eta^2} \quad - (3)$$

or

$$\Delta L \cdot \eta^2 \geq \frac{eLh\nu}{E_0s} \quad - (4)$$

We require both ΔL and η to be as small as possible (equivalent to large spatial resolution and high measurement accuracy) and thus we may regard the reciprocal of $\Delta L\eta^2$ as a performance figure of merit, F :-

$$F_{B/S} = \frac{E_0s}{eLh\nu}$$

In order to provide some feel for the implications let us take some 'typical' values for a silica fibre DOFS backscatter system :-

$$\begin{aligned} L &= 100 \text{ m} \\ E_0 &= 1 \text{ nJ} \\ n &= 5 \cdot 10^{14} \text{ Hz } (\lambda = 600 \text{ nm}) \\ s &= 5 \cdot 10^{-3} \end{aligned}$$

These give $F_{B/S} = 5.6 \cdot 10^4 \text{ m}^{-1}$

This implies that, for an accuracy of 1% ($\eta=0.01$) we have $\Delta L > 0.18\text{m}$.

(It should, however, be pointed out that the above calculation refers to 'single-pulse' performance, and significant improvement can result from integration over many pulses, if the consequent increase of measurement response time can be tolerated).

Suppose, however, that there is no necessity to rely on backscattered light. Consider the forward-scatter arrangement shown in fig 2. In this arrangement a continuous wave (CW) source is launched, at one end (F) of the fibre, into one of two possible modes T and R, say. These might be two propagation modes, two polarization modes, or even two separate cores within the same cladding. The important conditions which must obtain are that the two modes must be separately identifiable at the output from the fibre, and that light coupling between them must both be possible and dependent, in some way, on the external field to be measured (measurand). The mode into which the CW is launched will be labelled the 'filled' (in this case T) mode whilst the other is the 'free' (in this case R) mode.

An optical pulse is now launched into the other end (B) of the fibre in such a way as to allow it, whilst propagating in the opposite direction to the CW, to couple the latter from the 'filled' to the 'free' mode. If, as was required above, the coupling mechanism is modulated by the measurand in a deterministic way, then, by time-resolving the CW power level emerging from end B in the 'free' mode, one obtains the spatial distribution of the measurand field.

The important advantage which this method offers over the backscatter technique is that of increased received power level. There is no longer an optimum attenuation coefficient for a given fibre length, since one is not relying on backscatter (although the mode-coupling requirement might impose other limitations on the minimum attenuation allowable). After a length L the CW power will in this case be given by :

$$p(L) = p_0 \exp(-\alpha L)$$

Suppose that a fraction q of this light power is coupled from the filled to the free mode, by the passage of the counterpropagating pulse, in the absence of a measurand field. For a resolution length ΔL at distance L from the CW launch end, the coupled energy will be :

$$\delta E_L = q p_0 2\Delta L/c$$

(since α can now be very small). As before, if we require an accuracy of η , in the shot noise limit we may write :

$$(\delta E_L/h\nu) \geq 1/\eta^2$$

and thus, analogously to equation (3), we have :

$$\Delta L \geq ch\nu/2qp_0 \cdot 1/\eta^2$$

and the forward-scatter figure of merit is :-

$$F_{F/S} = \frac{2qp_0}{ch\nu}$$

In order to make a meaningful comparison between the two figures of merit we shall make the following assumptions :

(i) the peak power in the fibre is limited by the onset of undesirable non-linear effects and is the same for both cases. Thus :

$$P'_0 = E'_0 \cdot \frac{c}{\Delta L}$$

where the primed quantities represent the maximum values. (Here we have also assumed that the pulse width is equal to the resolution length which, again, represents the optimum condition).

(ii) Over the full length, L , of the DOFS system, the CW is totally coupled to the free mode. In this case :

$$q' = \frac{\Delta L}{L}$$

Inserting these assumptions the ratio of the optimum figures of merit is given by :

$$\frac{F'_{F/S}}{F'_{B/S}} = \frac{2e}{s}$$

For the typical value of the backscatter capture fraction, s , of $5 \cdot 10^{-3}$ we have :

$$\frac{F'_{F/S}}{F'_{B/S}} \approx 10^3$$

Thus, for a given accuracy of measurement (for example) the optimum resolution interval for the forward-scatter arrangement is reduced by three orders of magnitude, i.e. down to 0.18 mm. For the same resolution in the two cases, the accuracy of measurement in forward scatter is increased by a factor ~ 30 .

Clearly, a study of methods by which forward-scatter DOFS might be implemented must be worthwhile.

3. STRATEGY FOR FORWARD-SCATTER DOFS

The first forward-scatter (F/S) method for DOFS to be studied relied on a Raman interaction between a counterpropagating pulse and a CW probe in a low-birefringence fibre [5]. In this, the CW probe received Raman gain from the pulse, and this gain depended on the relative polarization states of the probe and the pulse, these, in turn, being dependent upon the strain distribution along the fibre (fig. 3). As a demonstration of the basic principle of F/S DOFS this was satisfactory, but it was not developed further since the signal processing required to determine the strain distribution was too complex for practical implementation. However, polarization methods are to be preferred since they are both very sensitive and independent (to first order) of fibre attenuation. High birefringence (hi-bi) fibres are now quite readily available. Such fibres possess a natural linear birefringence which allows good control over the propagation state of the propagating light, over long distances. Attention at King's College London recently has concentrated on the use of these fibres for DOFS.

The first attempt to use such fibres in DOFS involved a backscatter method [6,7] which was a variation on POTDR. In this method the propagating pulse, equally disposed in each of the two hi-bi eigenmodes, accumulated a linearly increasing phase difference between its two modal components as it propagated, and this was doubled for backscatter from any given point. By mixing the two backscattered eigenmodes signals on emergence, a frequency was generated, and the time dependence of this frequency mapped the distribution of birefringence along the fibre, corresponding to the pulse's passage along it (fig 4). Any external field capable of modifying that birefringence was mapped correspondingly. Whilst this method worked encouragingly well, it suffered still from that fact that it was a backscatter method, and thoughts turned towards attempts to embody the same, or a similar, idea in a forward-scatter arrangement.

The first thoughts along these lines involved the use of 'resonant' coupling. If a pulse propagating in a hi-bi fibre could be arranged to impose a suitable periodic perturbation with a spatial period equal to the hi-bi beat length (distance over which the differing polarization mode group velocities impose a phase difference of 2π between mode components) then this would lead to resonant coupling, from one mode to the other, of a counterpropagating CW probe. The birefringence could then be mapped via the coupling efficiency (level of coupled light) as a function of time.

4. MODE COUPLING IN HI-BI FIBRES

The primary feature responsible for the polarization-holding property of hi-bi fibre is that of the difference in group velocities for the two eigenmodes. Any perturbation which acts to couple light between the modes therefore, in general, will couple components with phases which average the resulting amplitude to zero over one beat length. Since this latter is typically of order a few mm, only perturbations with spatial variations on this scale will cause significant coupling. Clearly, a periodic perturbation which has a spatial period equal to a beat length will couple optimally, since the points of maximum coupling will always lead to fully constructive interference. The most obvious coupling perturbation is a strain which, acting in a direction at a non-zero angle to the eigenaxes, will induce an extra birefringence and thus effectively rotate the eigenaxes. The result is a coupling of each of the pre-existing eigen-components into the new axes directions, a coupling which is not, in general, reversed when the perturbation ends.

These ideas may be summarily quantified as follows :-

Suppose that the complex amplitude components in the two orthogonal linearly polarized eigenmodes of a hi-bi fibre are :

$$A_x = a_x \exp(i\beta_x z)$$

$$A_y = a_y \exp(i\beta_y z)$$

Suppose now that a perturbation acts so as to couple an amplitude fraction k from mode x to mode y per unit length. It follows that a fraction k^* (the complex conjugate of k) will be coupled from y to x (in order to conserve total power). Thus we may represent the coupling by means of a pair of coupled equations :

$$\frac{da_x}{dz} = ika_y(z)\exp(i\Delta\beta z)$$

$$\frac{da_y}{dz} = ika_x^*(z)\exp(-i\Delta\beta z)$$

where

$$\Delta\beta = \beta_y - \beta_x$$

Clearly, in order to solve these equations it is necessary to prescribe the dependence of k upon z . Suppose that k is periodic, with period L_p , ie.

$$k = k_0 \exp\left(\frac{i2\pi z}{L_p}\right)$$

$$k^* = k_0 \exp\left(-\frac{i2\pi z}{L_p}\right)$$

A solution of these equations now leads to the result that the fractional cross-coupled power over a distance L of fibre is given by

$$\chi = k_0^2 \left(\frac{\sin \alpha L}{\alpha} \right)^2 \quad - (4)$$

where :

$$\alpha = \left(k_0^2 + \left(\frac{\Delta\beta_0}{2} \right)^2 \right)^{\frac{1}{2}}$$

with

$$\Delta\beta_0 = \beta_y - \beta_x - \frac{2\pi}{L_p} = 2\pi \left(\frac{1}{L_B} - \frac{1}{L_p} \right)$$

L_B being the intrinsic fibre beat length. From this we see that the coupling is maximised when $L_B = L_p$ ($\Delta\beta_0 = 0$) under which condition

$$\chi = \sin^2 k_0 L \quad - (5)$$

Further, it is easy to show that, for an induced birefringence B_I with axes at angle θ to the intrinsic axes,

$$k_0 = \frac{B_I}{\lambda_0} \sin 2\alpha$$

coupled power as a function of position allows a measurement of the distribution of birefringence along the fibre, and hence also of any distributed field, such as stress, which modifies it.

5. KERR-EFFECT METHODS FOR IMPLEMENTING FORWARD-SCATTER DOFS

When an electric field is applied to an isotropic material (such as fused silica), linear birefringence is induced in the material, with the slow axis in the direction of the field and the fast axis orthogonal to it. The birefringence is given by :

$$B_k = \lambda_0 b E^2 \quad - (6)$$

where λ_0 is the vacuum wavelength, b the Kerr constant and E the electric field.

In the optical Kerr effect the electric field is that associated with an optical wave, so that the birefringence induced by an intense wave in a material may be probed via the effect it has on another wave, either co-propagating or counterpropagating.

Two F/S DOFS arrangements, which use the optical Kerr effect, have been explored:-

(i) FREQUENCY-DERIVED FORWARD-SCATTER DOFS

Frequency-derived backscatter DOFS has already been described in Section (3) and has also been reported in the literature [e.g. 6,7]. The forward-scatter version of this idea utilises the optical-Kerr effect.

Suppose that an intense optical pulse is launched into a hi-bi fibre, with equal power in each of the two eigenmodes. As the pulse propagates the two components will come into phase once per beat length and into antiphase at the intervening half beat lengths (fig. 5). The electric field of the resultant wave thus will maximise in a direction lying at $\pm 45^\circ$ to the intrinsic axes, every alternate half beat length. The Kerr-effect induced birefringence resulting from this field consequently will cause the resultant birefringence axes to rock around the intrinsic direction with a spatial period equal to the beat length.

Consider now a CW, with the same wavelength as the pulse, launched, again equally into the two eigenmodes, in the opposite direction to the pulse. When it encounters the pulse, the Kerr-induced rocking will produce optimal phase-matched coupling (since the rocking occurs naturally at the 'resonant' frequency), as a result of which probe power will be coupled from one mode to the other. When pump and probe are at the same wavelength there will be an exact correspondence in beat length which will maintain the coupled power constant as the pulse propagates down a fibre with uniformly distributed birefringence. However, if pump and probe are at different wavelengths the differing beat lengths will lead to the condition that optimum coupling will occur only when the rocking axes can couple in-phase probe components, i.e. with an effective beat-length given by L_e where

$$\frac{1}{L_e} = \frac{1}{L_1} - \frac{1}{L_2} ; L_e = \frac{\lambda_1 \lambda_2}{\Delta \lambda B_I} \quad (\Delta \lambda = \lambda_1 - \lambda_2)$$

From this we may conclude that the optimum coupling occurs at a 'beat' frequency given by :

$$f_D = c B_I \cdot \frac{\Delta \lambda}{\lambda_1 \lambda_2} \quad - (7)$$

where λ_1 is the wavelength of the pulse light, λ_2 that of the probe light, and L_1, L_2 the respective beat lengths; c is the velocity of light in the fibre and B_1 is the intrinsic birefringence of the fibre.

For small coupling, the power coupling efficiency, k^2 , is governed by [8] :

$$k^2 = \{ \sigma^2 / [\sigma^2 + (\theta/2)^2] \} \sin^2 \{ L_{\text{int}} [\sigma^2 + (\theta/2)^2]^{1/2} \} \quad (8)$$

where $\theta = (2\pi/L_e)$ is the dephasing parameter, and L_{int} is the interaction length. Also, the coupling coefficient σ is given by [9] :-

$$\sigma = \{ \pi B_k / 2\lambda_1 \} \quad (9)$$

where B_k is the optical Kerr-induced birefringence. As the wavelength of the pump is shifted with respect to the probe, a phase mismatch will appear between the coupled wave elements along the fibre. As a result, the net coupling would be reduced compared to the case where both sources have the same wavelength, as expected from equation (8). The pump power cannot be raised indefinitely to compensate for this, because of a limitation on the peak pump power in the fibre due to the onset of spectral broadening effects (e.g. Raman, Brillouin) which would further reduce the coupling efficiency. A large wavelength shift between the pump and probe beams therefore cannot be achieved without paying a substantial penalty in terms of the coupling efficiency. Equation (7) shows that this, in turn, limits the tuning range of the derived probe frequency. To avoid this problem the pump pulse should be short compared with the spatial beat length between the polarization states of the pump and probe beams, so as to avoid the 'smoothing' effect caused by the probe pulse embracing many beat lengths, i.e. to keep L_{int}/L_e (in equation (8)) small. The experimental setup is illustrated in fig (6). The fibre used was 24m long with an elliptical core (supplied by Andrew Corporation) and was single mode at 633nm, where it exhibited a beatlength of 4 mm. The pump pulses were generated by a dye laser pumped by a Q-switched, frequency-doubled Nd: YAG laser. Pulses of 8 ns (FWHM) maximum duration were generated with a repetition rate of 50 Hz. To allow useful differences between the pump and probe wavelengths, the duration of the pump pulses was required to be shorter than the pulse width actually available from the dye laser. Accordingly a fast optical shutter was used to provide a sufficiently short pulse. The pump beam was chopped by a fast Pockels cell to provide pulses of 2 ns (FWHM) and was circularly polarized by the quarter wave plate so as to excite equally the two eigenmodes of the fibre. The probe was provided by a cw Argon-pumped dye laser which was counter-propagating with respect to the pump, and linearly polarized at a small angle to the fibre's birefringence axes, with a launched power of ~ 300 mW. In principle the strongest probe signal should be provided when the eigenmodes are equally excited by a launched polarization set at 45° to the fibre's principal axes. The signals would be then superimposed on a high mean received power. However, an avalanche photodiode detector was used, and this rendered high mean signal levels undesirable. After reflection from a beamsplitter at near-normal incidence, the probe beam was analysed with a Glan Thompson analyser. A monochromator was placed before the avalanche photodiode detector in order to block the large pulse predominantly produced by the front face reflection from the fibre. This pulse otherwise would have saturated the input amplifier. The pump and probe beams were set at various wavelength differences up to 2.4 nm apart, generating derived signal frequencies up to ~ 200 MHz. The signals were recorded and analysed using a computer-interfaced digital storage oscilloscope which was used to average the results from 256 pump pulses. The averaging process occupied approximately 10 seconds.

For the length of fibre used in the experiment, the spectrum began to broaden when the first stimulated Raman line was generated. This occurred at a pulse energy of about 35 nJ. The experimentally achieved coupling efficiency was about 1%. The variation of the derived frequency with wavelength

offset was measured by the following method: the pump and probe were initially set at the same wavelength of 646 nm. Then, by tuning the pump wavelength with respect to the probe, the required wavelength shift was set. An example of a derived frequency signal averaged over 256 pump pulses is shown in fig (7). The wavelength shift between the pump and probe in this measurement is 1.5 nm and the corresponding derived frequency is 71MHz. The measured signal to noise ratio was 19.3 dB. The experimentally-observed and theoretically-calculated relationships between the frequency and wavelength shift are shown in fig (8). This figure shows the expected linear trend connecting the derived frequency with the wavelength shift. There was good agreement between the theoretical prediction represented by the line in the figure, and the experimental values represented by the points, when the wavelength of the probe was longer than that of the pump, but this relationship did not hold for the reverse case. Further tests made for the reverse case also showed a linear trend, but with a different slope. This may be due to systematic experimental error, but this remains to be confirmed. The tuneable frequency range offering strong signals was limited. This agrees closely with the theory given by equation (8), in that, for a 2ns pump pulse, the first zero of the coupling response was expected to occur at a wavelength offset of ~ 3.2 nm, and from equation (7) the equivalent signal frequency would then be ~ 200 MHz.

Using the novel technique presented here, the spatial variation of the birefringence of a polarization maintaining fibre can be measured remotely in a short time, and, since the signal is in the form of a frequency, it is immune from the common error sources present in intensity - coded systems. Any change in the applied stress or ambient temperature will tend to change the local birefringence and will therefore be indicated by a shift in the frequency due to the external perturbation. Thus this technique may be applied to implement a distributed optical fibre sensor. In this application the tuneability of the derived frequency could provide some extra flexibility in the system design.

(ii) POLARIZATION-STATE DEPENDENT KERR EFFECT FORWARD-SCATTER DOFS

In this second method the emphasis presently is on the spatial location of a perturbation rather than the measurement of its magnitude, although suitable processing is capable, in principle, of revealing the latter. In its present form it is capable of providing good spatial resolution and rapid response for application to, for example, intrusion monitoring or vehicle location.

The optical arrangement employs a length of polarization maintaining fibre carrying two counter-propagating beams. A CW probe beam is launched from one end of the fibre so as to excite equally the two eigenmodes, and the polarization state of this beam is detected at the far end of the fibre by means of a beamsplitter and analyser oriented at forty-five degrees to the birefringence axes. An intense, pulsed, pump beam is launched on one of the birefringence axes. This arrangement is similar to the well-known Kerr-effect shutter system [10]

As in the Kerr shutter, the pump pulse causes a phase shift between the eigenmodes of the probe beam, leading to a change in the output polarization state of the probe. This is detected as a sharp change in the probe intensity passed by the analyser when the pump is initially launched into the fibre.

If, now, a force acts at an angle to the axes along a section of fibre, coupling of the pump light to the other axis will occur, and the Kerr effect on the probe will thus be modified. The probe light itself will also experience mode coupling, which will further modify the output polarization state. The actual change which occurs will depend, inter alia, on the states of polarization of the beams as they enter the perturbed region and thus, unless the birefringence perturbation is very small compared with the intrinsic birefringence, there will exist a mutual dependence of effects from different measurement locations, which only fairly complex signal processing would be able to resolve. However, it is clear that for any change in the direction of birefringence axes consequent upon the perturbation by a

measurand, there will, in general, result a change in optical Kerr effect. A differentiated signal thus will, at least, indicate differential features of the measurand distribution, even though a fully quantified spatial distribution is more elusive.

The fibre used in the experiments [11] was a mono-mode high-birefringence fibre, manufactured by Andrew Corporation, with a diameter of $67\mu\text{m}$, attenuation of 35dB/km at 633nm and core to cladding refractive index difference $\Delta n = 0.032$. The length of the fibre was about 100m . The arrangement of the experiment is shown in Fig (9). Pump pulses (617nm) of 8ns (FWHM) duration were generated in a dye laser with a repetition rate of 50Hz . These pump pulses were launched on to one of the birefringence axes of the fibre with the help of a halfwave plate and with a peak power of 3W measured at the output end of the fibre. The linearly polarized probe beam of wavelength 633nm , from a He-Ne laser, was launched into the fibre at 45° to the birefringence axes. On emergence, the probe beam was directed by a beam splitter to the detector, via the polarization analyser; its average power at the detector was about $25\mu\text{W}$. The He-Ne laser and the detector were protected from the pump light by use of band-pass filters at 633nm . Force was exerted by pressing metal rods on the fibre. The received signals were recorded, averaged and differentiated using the functions of the digital storage oscilloscope.

In the absence of any measurand-induced perturbation the Kerr effect of the pulse is to modify the local value of birefringence as it propagates, a modification which is sensed by the probe beam as a phase shift between the eigenaxes, and which is, in principle, constant for the duration of the pulse's passage through the fibre. The effect of this phase shift on the optical signal passing through the analyser is shown in fig (10). In practice, the slow fall in the value of the phase shift is due to the attenuation of the pump pulse with distance along the fibre. Fig (10) also shows the effect of differentiating this signal with respect to distance.

Fig (11) the fluctuating analyser signal when the fibre was perturbed at two points, and its differential with respect to distance. The points at which the weights were applied are clearly evident. Such a system, even as it stands, could be used as an intruder alarm or as an indication of anomalous disturbance of almost any kind.

Thus is demonstrated the use of the optical Kerr effect to determine the locations of discrete mode coupling points space along a polarization maintaining fibre. Differentiation of the received signal with respect to time provides a simple way to reduce confusing interactions when multiple coupling points are present. Further work on this method is continuing, with a view to developing practical real time processing and theoretical analysis of the potentialities of the technique.

CONCLUSIONS

Forward-scatter non-linear DOFS offers significantly improved performance over backscatter systems. The enhanced detector SNRs imply the possibility of better than 1% measurement accuracy with spatial resolutions of a few millimetres, and rapid response. The primary disadvantage is that higher-power sources are required in order to access the non-linear optical regime.

Two systems in this class have been explored using the optical Kerr-effect. Both systems are basically polarimetric in form and rely on the properties of hi-bi fibre.

These systems are capable of further development, and others are possible.

This class of DOFS methods offers much promise for practical DOFS systems in a variety of industrial applications, including 'smart' material structures.

ACKNOWLEDGEMENTS

The work described above has benefited from contributions from a number of colleagues, most notably Dr. V. A. Handerek, Mr S U. Ahmed, Mr I. Cokgor and Mr F Parvaneh. The work has been supported by the UK's SERC, the Royal Society and the UK Optical Sensor Collaborative Association (OSCA).

REFERENCES

1. Rogers A. J. 'Distributed Optical-fibre Sensors for the Measurement of Pressure, Strain and Temperature' Phys. Rep. Vol 169, No. 2, 1988, pp 99-143.
2. Culshaw B. 'Distributed and Multiplexed Fibre-optic Sensor Systems' Proc. NATO Adv. Study Inst (Erice, Italy) 1986 (Nijhoff, The Hague).
3. Handerek V. A. and Rogers A. J. 'Sensor System Architectures for Spatially-resolved Dynamic Strain Measurement Using Optical Fibres', Proc. 1st European Conference on Smart Structures and Materials, Univ. of Strathclyde, May 1992.
4. Rogers A. J. 'Point and Distributed Polarimetric Optical-fibre Sensors' Int J. Opt. Sensors, Vol 1, No 6, 1986, pp 457-472.
5. Farries M. C. and Rogers A. J. 'Distributed Sensing Using Stimulated Raman Action in a Monomode Optical Fibre', Proc. 2nd Int. Conf on Optical-fibre Sensors, Stuttgart, 1984, pp 121-132.
6. Handerek V. A., Parvaneh F. and Rogers A. J. 'Frequency-derived Distributed Optical-fibre Sensing : Signal Frequency Downshifting', Elect. Lett, Feb. 1991, Vol 27, No 5, pp 394-396.
7. Rogers A. J. and Handerek V. A., 'Frequency-derived Distributed Optical-fibre Sensing: Rayleigh Backscatter Analysis', Appl., Opt. Vol 31, No. 21., 1992, pp 4091-4095
8. Ahmed S. V., Handerek V. A., Rogers A. J. 'Phase-matched Polarization Coupling in High-birefringence Fibres through the Optical Kerr Effect', Opt. Lett. Vol 17, No 9, 1992, pp 643-645.
9. Parvaneh F., Valente L. C. G., Handerek V. A. and Rogers A. J. 'Forward-scatter Frequency-derived Distributed Optical-fibre Sensing Using the Optical Kerr Effect', Elec. Lett. June 1992, Vol 28, No. 12, pp 1080-1082.
10. Dziedzic S. M., Stolen R. and Askhin A., 'Optical Kerr Effect in Long Fibres', Appl. Opt. Vol. 20, 1981, pp 403-406.
11. Handerek V. A., Rogers, A. J. and Cokgor I., 'Detection of Localized Polarization Mode Coupling using the Optical Kerr Effect', Proc. 8th Int. Conf. on Optical fibre Sensors (OFS 8), Monterey, California, January 1992, pp 250-253.

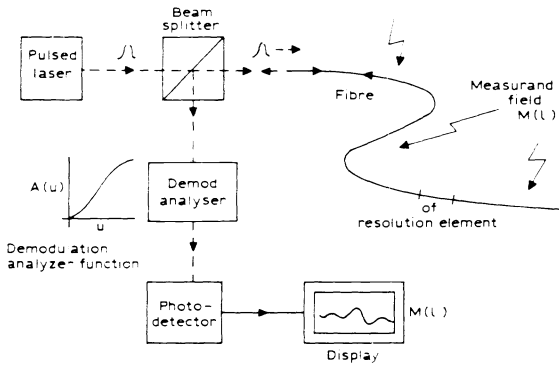


Fig 1. OTDR for Distributed Measurement

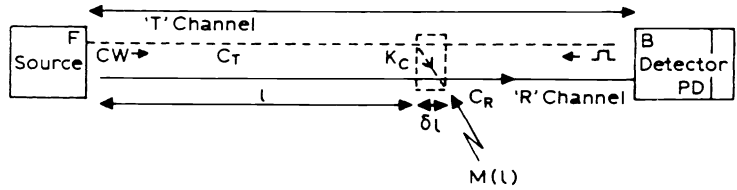


Fig 2. Schematic for Forward-scatter DOFS

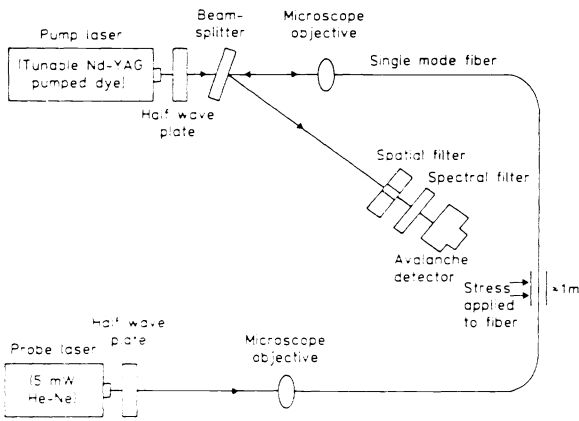


Fig 3. Raman Gain Forward-scatter DOFS

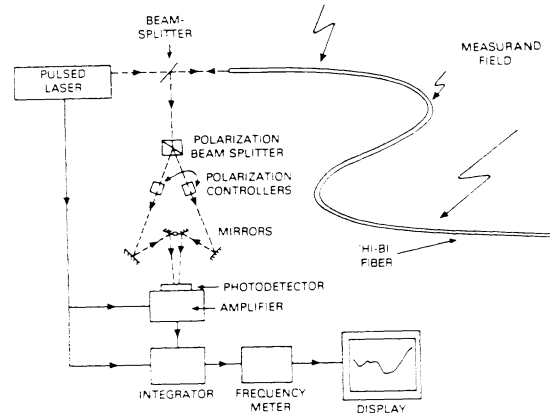


Fig 4. Frequency-derived Backscatter DOFS

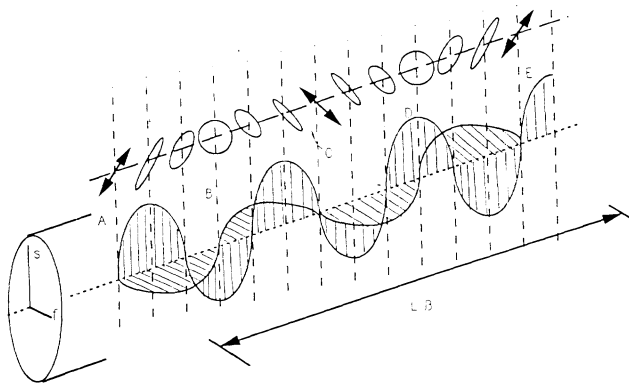


Fig 5. Evolution of Polarization State in Hi-Bi Fibre

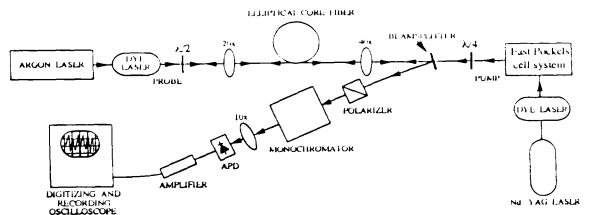


Fig 6. Experimental Arrangement for Optical Kerr Effect Coupling DOFS

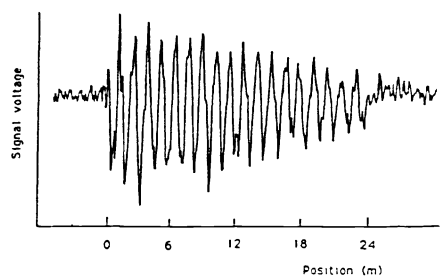


Fig 7. Derived-frequency Signal from Optical Kerr Effect DOFS

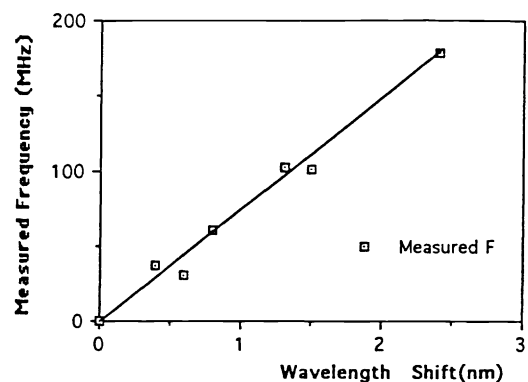


FIG 8. Derived Frequency versus Pump-probe Wavelength Difference

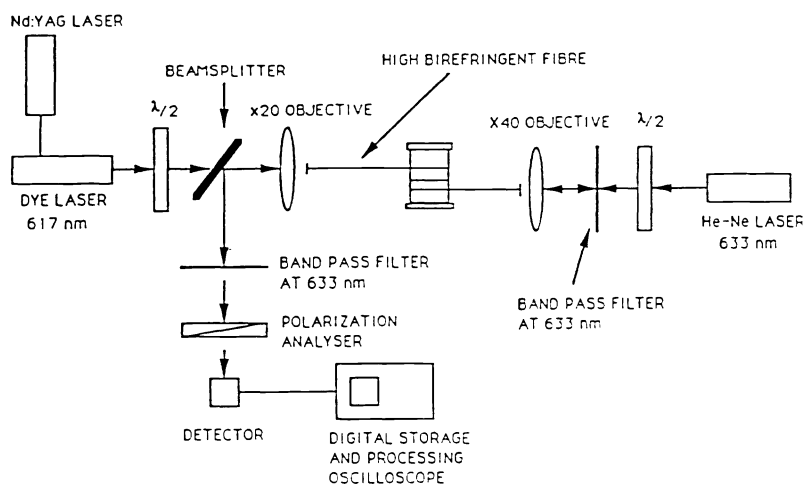


Fig 9. Experimental Arrangement for Polarization-state Dependent Kerr Effect DOFS

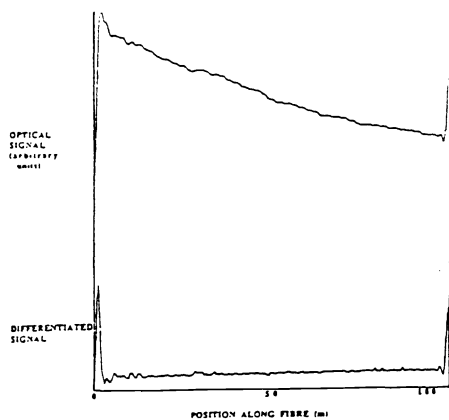


Fig 10. Unperturbed Signals

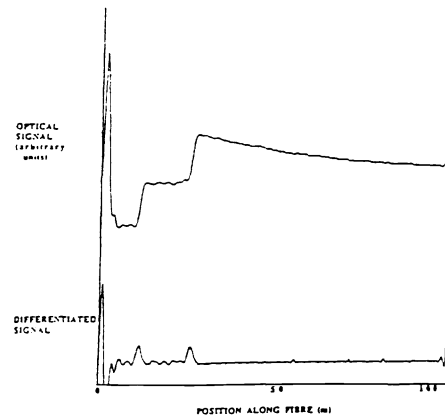


Fig 11. Signals with Two Points of Stress Perturbation